

Section 9

**Development of and studies with
coupled ocean-atmosphere models**

The Impact of Ocean Conditions on the Hurricane Blanca (2015) Forecasts with a Coupled Model

Hyun-Sook Kim*, Dan Iredell, Samuel Trahan, and Avichal Mehra

*IMSG/Environmental Modeling Center, NCWCP, College Park, Maryland 20740, USA

hyun.sook.kim@noaa.gov

1. Introduction

The 2015 North Eastern Pacific hurricane season was affected by the strongest El Niño-Southern Oscillation (ENSO) ever recorded, setting a record long season and an all-time large number of hurricanes (<http://www.nhc.noaa.gov/text/MIATWSEP.shtml>). By May, the SST anomaly already exceeded 2°C (http://www.cpc.ncep.noaa.gov/products/Epac_hurr/Epac_hurricane.html) in the Nino index areas 1 and 2. Consequently, the Main Development Region (MDR) was set for favorable conditions even before the official season started. The season's second Tropical Cyclone (TC) Blanca formed on 12Z May 31, centered (102.2°W, 12.0°N) in the MDR. Over the next 78 hours, the storm intensified to a cat 4 hurricane (125 kts), and strengthened by 60 kts during a 24 hour period (18Z June 2–18Z June 3). Of specific interest, however, was its quasi-stationary translation speed of 0.5-1.5 ms⁻¹ during this rapid intensification period. Models used for numerical guidance by the NHC (National Hurricane Center) estimated a SST cooling of $O(18^{\circ}\text{C})$, while predicting maximum winds that were weaker by 40 kt than the NHC's observed values. This is a baroclinic response of the thermodynamic coupling between SST, deep convection and surface wind. This feedback can further accelerate if a storm moves more slowly. Here we present evidence of the impact of oceanic conditions on intensity forecasts, using a Hurricane Weather Research Forecast (HWRF) model coupled to the Princeton Ocean Model (POM) (which is NHC's operational guidance), and coupled to the HYbrid Coordinate Ocean Model (HYCOM) system. The ocean models solve the same 3D governing, free-surface, primitive equations on a similar 1/12° resolution. The major differences between the POM and HYCOM are, respectively: a) initialization from climatology vs. the Navy Coupled Ocean Data Assimilation (NCODA)-HYCOM analysis; b) climatology vs. NCEP RTOFS forecasts for boundary conditions; c) Mellor-Yamada 2.5 closure vs. KPP mixing physics; and d) 24 sigma vs. 36 hybrid level-isopycnal vertical layers.

2. Simulation Results

Comparisons of track and intensity forecasts for the 00Z cycle on June 3, between HWRF-HYCOM (henceforth H5Y5), HWRF-POM (henceforth HCTL) and the “best track” (BT) are shown in Fig. 1. The H5Y5 and HCTL tracks both have an eastward bias with respect to BT, with very little difference between them (Fig. 1A). However, each model under-predicted the maximum wind intensity (V_{max}) (Fig. 1B) though H5Y5 exhibits better skill than HCTL, with error reductions up to 30 kt. The V_{max} at 24 h (vertical line in Fig. 1B), for instance, is 93 kt vs. 63 kt for H5Y5 and HCTL, respectively. Sea Surface Temperature (SST) cooling at that forecast hour is 7.7°C for H5Y5, and is 1.1°C higher than that predicted by HCTL (not shown). This somewhat contradicts a typical thermodynamic coupling relationship.

Comparisons of the 24-h upper ocean structure in near field show that HCTL simulates shallower mixed layer (~40 m) for HCTL than the H5Y5 depth (> 80 m). Also, the mixed layer temperature for HCTL is cooler by <1°C and <3°C for 40 m and 80 m, respectively, than the H5Y5 estimates. An outstanding difference, however, is the presence of warm eddies at depths (< 95 m) for H5Y5 runs.

The pre-storm ocean conditions are drastically different. Fig. 3 shows ocean heat content (OHC) for an initial time of 18Z May 31, which indicates the structure of the upper layer. The OHC differences are not only in spatial variability, including warm eddies and filaments, but also the magnitude. The overall OHC difference between HCTL and H5Y5 is more than 50 kJcm⁻², and the largest difference exists in the area surrounding Blanca. The maximum available OHC is ~94 kJcm⁻² at (105°W, 12°N) for HCTL vs. ~145 kJcm⁻² for H5Y5, and it locates in the surrounding area of Blanca in the form of meso-scale eddy. Comparisons against the Argo observations (Table 1) support the difference. Specifically, HCTL under-estimates OHC at low latitudes by ≤ 54.4 kJcm⁻² and over-estimates it by 8.9 kJcm⁻² at higher latitudes. For comparison, the H5Y5 OHC exhibits similar magnitudes to those observed, with mean and RMS differences of 4.1 and 2.7 kJcm⁻², respectively. H5Y5 provides significantly larger and more accurate initial OHC estimates than HCTL. The representation of realistic pre-storm upper oceanic conditions with H5Y5 leads to compelling improvements in its hurricane intensity forecasts (Fig. 1B).

3. Concluding remarks

The study of temperature and OHC simulations from operational and experimental coupled HWRF systems suggests that the ocean component of the operational model (POM) provides less accurate upper ocean conditions for Hurricane Blanca. The reason is that POM is initialized from a climatological temperature and salinity structure, and daily GFS SST assimilation is insufficient in correcting the upper structure to a realistic representation. This is implied in the OHC comparisons against observations, showing that POM underestimates OHC by as much as 54.5 kJcm^{-2} . In contrast, RMS differences for OHC in HYCOM are small (2.7 kJcm^{-2}), and the model correctly captures most subsurface features. This study demonstrates the importance of ocean initial conditions to hurricane forecasting, and that the climatology-based initial conditions are ill-equipped to represent the correct heat potential source in an intensifying tropical cyclone.

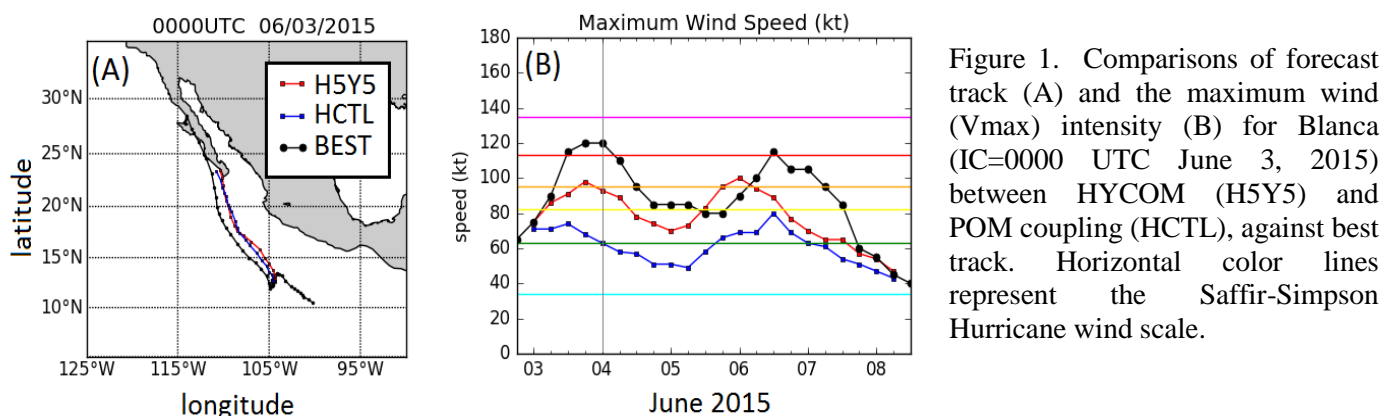


Figure 1. Comparisons of forecast track (A) and the maximum wind speed (V_{max}) intensity (B) for Blanca (IC=0000 UTC June 3, 2015) between HYCOM (H5Y5) and POM coupling (HCTL), against best track. Horizontal color lines represent the Saffir-Simpson Hurricane wind scale.

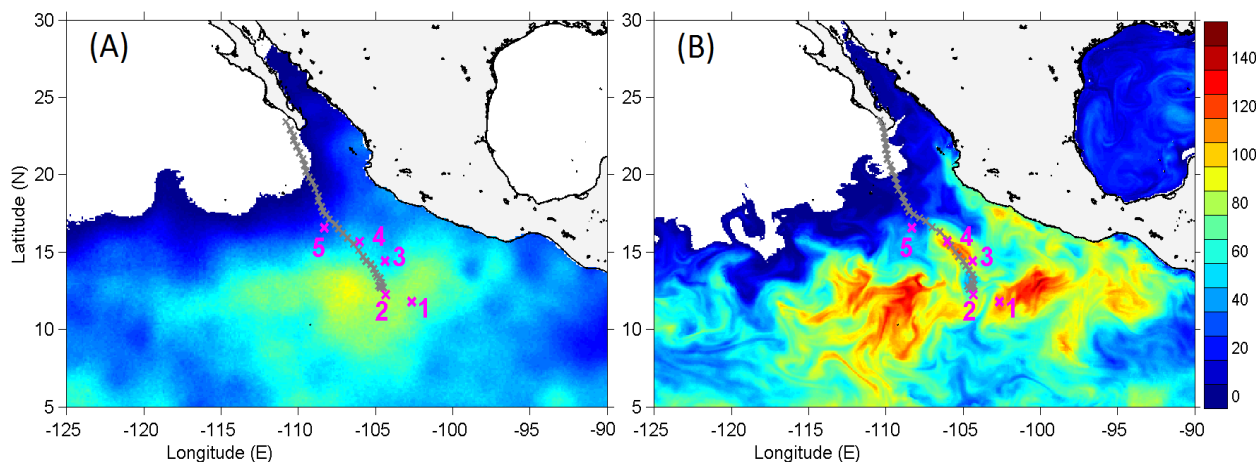


Figure 2. Ocean heat content at initial time (18Z May 31) for HCTL (A) and H5Y5 (B), with superimposed forecast track (IC=00Z June 3). Numbers on/around the track represent Argo positions (see Table 1).

Table 1. Comparisons of ocean heat content (OHC) for a pre-storm period against Argo estimates. The uncertainty of the Argo OHC is 1.5 kJcm^{-2} . Units are kJcm^{-2} .

Argo		HCTL			H5Y5						
#	ID	Julian day	Lon. ($^{\circ}$ W)	Lat. ($^{\circ}$ N)	OHC	Lon. ($^{\circ}$ W)	Lat. ($^{\circ}$ N)	Δ OHC	Lon. ($^{\circ}$ W)	Lat. ($^{\circ}$ N)	Δ OHC
1	4901510	23891.45	102.66	11.79	123.0	102.70	11.86	-54.5	102.64	11.91	5.6
2	4901509	23890.34	104.33	12.23	118.2	104.33	12.20	-38.3	104.32	12.23	0.0
3	4901511	23889.79	104.38	14.41	105.1	104.33	14.38	-58.9	104.40	14.41	8.2
4	4900842	23885.86	106.03	15.67	84.7	106.06	15.63	-35.9	106.00	15.64	4.0
	4901638	23893.26	108.30	16.56	29.2	108.26	16.55	8.9	108.32	16.56	2.8

The effect of predicted oceanic conditions on the assimilation of Typhoon Sinlaku (2008)

Akiyoshi Wada* and Masaru Kunii

*Meteorological Research Institute, Tsukuba, Ibaraki, 305-0052, JAPAN

awada@mri-jma.go.jp

1. Introduction

This report follows the work of Wada and Kunii (2014, 2015) that described the development of a regional coupled atmosphere-ocean assimilation system based on the local ensemble transform Kalman filter (LETKF) and the nonhydrostatic atmosphere model (NHM) coupled with the multilayer ocean model and the third generation ocean surface-wave model (Wada et al., 2010). The coupled system includes the effect of sea spray. The sea-spray parameterization helped tropical cyclone (TC) intensification by increasing turbulent heat fluxes near the atmospheric surface-boundary layer as described in Wada and Kunii (2015).

In the previous works of Wada and Kunii, ocean predictions calculated in a forecasting part of the coupled system were not used in both the analysis and the following prediction. The purpose of this study is to introduce the ocean predictions into the following calculation in order to understand the effect of oceanic variations on the analysis of the TC. This study addresses Typhoon Sinlaku (2008) as a case study, which is the same as considered in Wada and Kunii (2014, 2015).

2. Experimental design

Figure 1 displays a schematic diagram of the revised NHM-LETKF assimilation system. It uses daily oceanic reanalysis data calculated by the Meteorological Research Institute multivariate ocean variational estimation (MOVE) system (Usui et al., 2006) only at the initial step. After that, restart data calculated by the ocean and wave models were used as input for the following predictions in the next cycle. The restart data were used for conducting numerical simulations as a sequential job. Therefore, the ocean is continuously predicted through the entire assimilation period without taking into account the influence of in situ observations and oceanic reanalysis data.

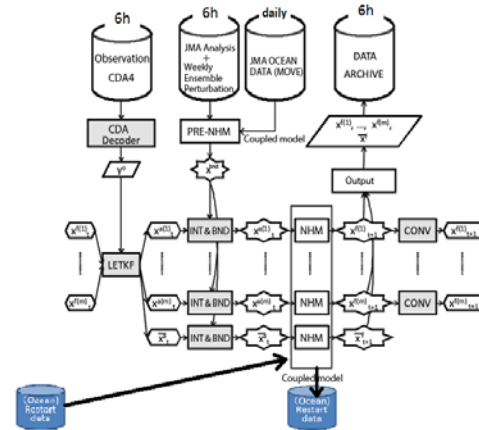


Figure 1 Schematic diagram of NHM-LETKF coupled with the atmosphere-wave-ocean model in the prediction part with oceanic reanalysis data.

The experimental design was almost the same as in Wada and Kunii (2015). The coupled atmosphere-wave ocean model consists of the NHM, the third generation ocean-wave model, and a multilayer ocean model (Wada et al., 2010). The analysis component of the LETKF system was the same as in Kunii (2014). The ocean (wave conditions) was assumed to be motionless only at the initial time.

The analysis and prediction of the storm were performed over a ~3600 km x ~1900 km computational domain with a horizontal grid spacing of 15 km. The system had 40 vertical levels with variable intervals from 40 m for the near-surface layer to 1180 m for the uppermost layer. The system had maximum height approaching ~23 km. The analysis period was from 1200 UTC 1 September to 1800 UTC 19 September in 2008. The number of ensemble members was 50. Wind stresses from the atmosphere to the ocean were tuned to be twice larger in the ocean model since the horizontal resolution (15 km) was relatively coarse for tropical cyclone simulations and thus the atmosphere model predicted relatively weak wind stresses. Table 1 shows experimental design.

‘Atmos’, ‘Wave’ and ‘Ocean’ means a component of forecasting model. ‘Restart’ means that predicted ocean waves and ocean components are propagated in the next cycle. This is only used in ‘REST’. The left vertical column in Table 1 indicates the name for each experiment. ‘CNTL’ used the NHM, ‘Wave’ used the NHM-wave-coupled model, and ‘FULL’ and ‘REST’ used the NHM-wave-ocean coupled model.

3. Results and concluding remarks

Figure 2 presents the results of ensemble mean TC track positions every 6 hours with Regional Specialized Meteorological Center (RSMC) Tokyo best track (BT). The effect of ocean coupling in the ensemble mean TC track is negligible among the four experiments except for an early phase of Typhoon Sinlaku, corresponding to the genesis phase. On the mid-latitude TC, the ensemble mean TC track is almost the same among the four experiments.

Table 1 Experimental design

Exp./Model	Atmos.	Wave	Ocean	Restart
CNTL	○	×	×	×
WAVE	○	○	×	×
FULL	○	○	○	×
REST	○	○	○	○

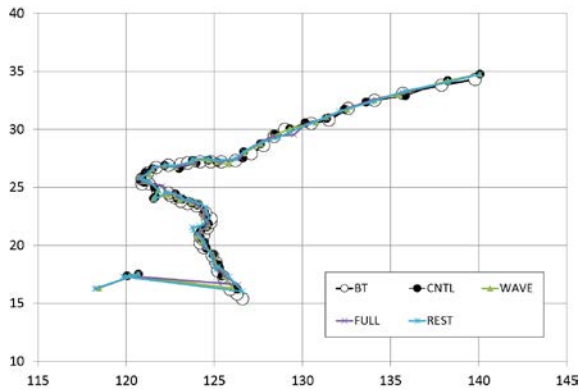


Figure 2 The results of ensemble mean TC track. BT indicates RSMC Tokyo best track positions every 6 hours.

Figure 3 shows the evolution of ensemble mean TC central pressures with RSMC Tokyo best-track central pressure. The effect of ocean waves (experiment WAVE) on the changes in ensemble mean central pressure is found during the intensification phase around 11 September, compared with those in CNTL. The intensification in FULL is similar to that in WAVE: The difference in the ensemble mean central pressure between CNTL and FULL is small. The result is different from the previous results reported in Wada and Kunii (2014, 2015) because the effect of turbulent heat fluxes on sea surface cooling induced by the typhoon was excessive in the previous coupled system. The current system improves the process based on the original coupled model (Wada et al., 2010).

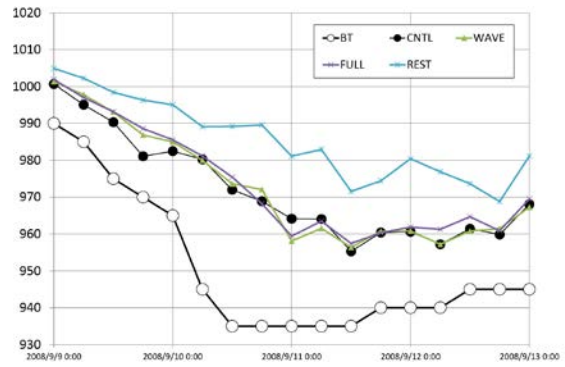


Figure 3 As in Fig. 2 except for ensemble mean TC central pressure.

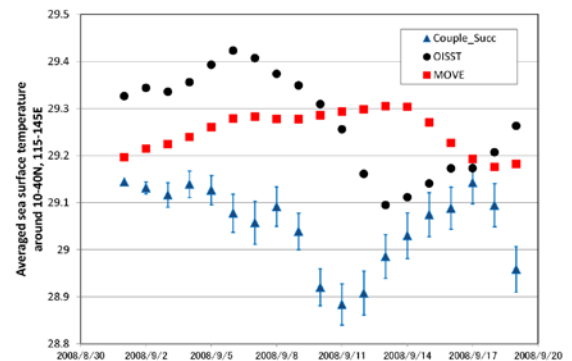


Figure 4 Evolutions of sea surface temperature averaged over the computational domain obtained from REST, MOVE and OISST.

Figure 4 shows the evolution of sea surface temperature averaged over the computational domain obtained from REST together with the average sea surface temperatures obtained from MOVE and OISST (<http://www.remss.com/>). The change in sea surface temperature is well reproduced in REST against that in MOVE with reference to that in OISST.

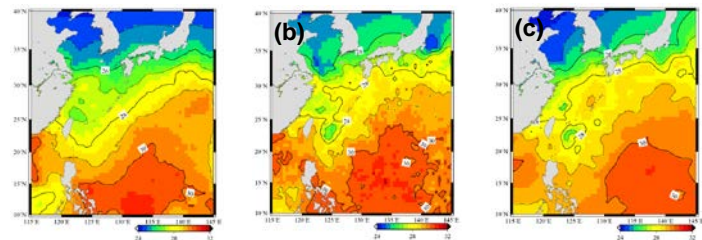


Figure 5 Horizontal distributions of sea surface temperature at 18 UTC on 19 September obtained in (a) REST, (b) OISST (<http://www.remss.com>)

Figure 5 displays the horizontal distribution of sea surface temperature at 18UTC on 19 September and the horizontal distributions of daily sea surface temperature in OISST and MOVE. The horizontal distribution of the sea surface temperature in MOVE is similar to that in OISST and is different from that in REST particularly in the location of Sinlaku induced sea surface cooling.

Therefore, the use of predicted oceanic conditions are able to change the prediction of TC intensity. This suggests that errors of ocean predictions do affect the accuracy of TC intensity analysis if oceanic values such as water temperatures are not controlled by observations. In order to improve the representation of the distribution of sea surface temperature, it should be dealt with control variables in the coupled assimilation system.

Acknowledgement

This work was supported by MEXT KAKENHI Grant Number 25106708 and by JSPS KAKENHI Grant Number 15K05292.

References

- Kunii, M. (2014). Mesoscale data assimilation for a local severe rainfall event with the NHM-LETKF system. *Weather and Forecasting*, (2013). <http://dx.doi.org/10.1175/WAF-D-13-00032.1>.
- Kunii, M. and Miyoshi, T. (2012). Including uncertainties of sea surface temperature in an ensemble Kalman filter: a case study of Typhoon Sinlaku (2008). *Weather and forecasting*, 27(6), 1586-1597.
- Usui, N., S. Ishizaki, Y. Fujii, H. Tsujino, T. Yasuda and M. Kamachi (2006). Meteorological Research Institute multivariate ocean variational estimation (MOVE) system: Some early results. *Advances in Space Research*, 37(4), 806-822.
- Wada, A., N. Kohno and Y. Kawai (2010). Impact of wave-ocean interaction on Typhoon Hai-Tang in 2005. *SOLA*, 6A, 13-16.
- Wada, A. and M. Kunii (2014). Introduction of an atmosphere-wave-ocean coupled model into the NHM-LETKF. *CAS/JSC WGNE Res. Activities in Atm. And. Oceanic Modelling*, 44, 9.03-9.04.
- Wada, A. and M. Kunii (2015). The impact of a sea-spray parameterization on the assimilation of Typhoon Sinlaku (2008) *CAS/JSC WGNE Res. Activities in Atm. And. Oceanic Modelling*, 45, 9.08-9.09.

Idealized storm evolution and the difference between the eastern and the western North Pacific calculated by an atmosphere-wave-ocean coupled model

Akiyoshi Wada

Meteorological Research Institute, Tsukuba, Ibaraki, 305-0052, JAPAN

1. Introduction

Previously, Wada et al. (2012) reported that the relationship between maximum tropical cyclone (TC) intensity and tropical cyclone heat potential (TCHP) accumulated from the genesis to first reaching the minimum central pressure (MCP) differed between the eastern and western Pacific. Relatively high accumulated TCHP was required for reaching a certain value of MCP in the western Pacific. In other words, TCs can intensify in the eastern Pacific more easily. In order to verify the difference of TC evolution and the maximum intensity, idealized numerical experiments were performed by using an atmosphere-wave-ocean coupled model (Wada et al., 2010) with an idealized TC-like vortex (see Wada, 2009).

2. Model and experimental design

The atmospheric initial conditions were provided by the global objective analysis of the Japan Meteorological Agency on a horizontal grid with a spacing of approximately 20 km. The date at the initial integration time was 00 UTC on 14 September in 2009. The computational domain centered at 16.0°N and 148.8°E in the experiment for the western North Pacific storm, and at 16.0°N and 108.5°W for the eastern North Pacific storm. At that time, Typhoon Choi-wan existed around the center position in the western North Pacific, whereas there was no TC in the eastern North Pacific. Figure 1 shows vertical profiles of potential temperature, equivalent potential temperature and saturated equivalent potential temperature in the eastern North Pacific (Fig. 1a) and those in the western North Pacific (Fig. 1b) averaged over the computational domain for each experiment. The middle troposphere was relatively dry in the eastern North Pacific at the initial time. TC-like vortex calculated based on Wada (2009) was introduced at the initial time.

A coupled atmosphere-wave-ocean model based on a nonhydrostatic atmosphere model, the third generation ocean wave model and a multilayer ocean model (Wada et al., 2010) was used in this study. The time step was 6 seconds. The domain covered 1200 x 1200 km² with a horizontal grid spacing of 1.5 km. The number of the vertical layer was 40 with variable intervals from 40 m at the lowermost layer near the surface to 1180 m at the uppermost layer, and a top height of nearly 23 km. The standard longitude of map projection for Lambert conformal projection was 120°W in the experiment for the eastern North Pacific storm, while it was 140°E for the western North Pacific storm. The Coriolis parameter was assumed to be constant (4.0×10^{-5}). The environment was assumed to be motionless.

Table 1 shows the list of numerical experiments. A half were performed by the coupled model, while the rest was performed by the atmosphere model. Two roughness schemes, Taylor and Yelland (2001) and Smith (1992) were respectively used for each experiment. In all experiments, a sea spray parameterization (Bao et al. 2000) was used. The sensitivity of rainpower effect (Sabuwala et al., 2015) on the evolution of TC-like vortex was additionally examined in the series of numerical experiments. The program for the effect was coded in the atmospheric boundary layer scheme on the atmosphere model.

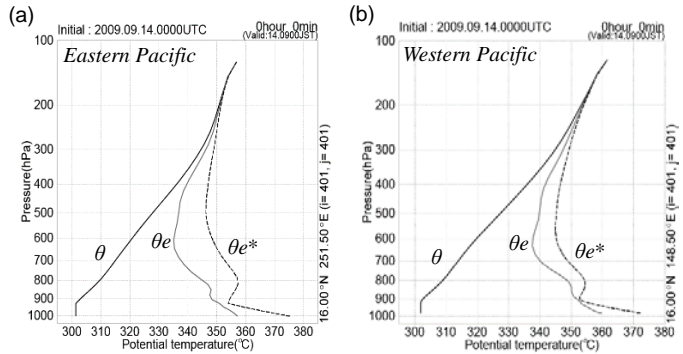


Figure 1 Initial vertical atmospheric profiles of potential temperature (θ : black solid line), equivalent potential temperature (θ_e : gray solid line) and saturated equivalent potential temperature (θ_{e^*} : dashed line) (a) in the eastern North Pacific and (b) in the western North Pacific.

Table1 List of numerical experiments.

Acronyms	Area	Ocean/Wave	Roughness length scheme	Rainpower effect
EAST_TY_A	Eastern Pacific	No	Taylor and Yelland (2001)	No
EAST_TY_AWO	Eastern Pacific	Yes	Taylor and Yelland (2001)	No
EAST_SM_A	Eastern Pacific	No	Smith(1992)	No
EAST_SM_AWO	Eastern Pacific	Yes	Smith(1992)	No
WEST_TY_A	Western Pacific	No	Taylor and Yelland (2001)	No
WEST_TY_AWO	Western Pacific	Yes	Taylor and Yelland (2001)	No
WEST_SM_A	Western Pacific	No	Smith(1992)	No
WEST_SM_AWO	Western Pacific	Yes	Smith(1992)	No
EAST_TY_A_RPW	Eastern Pacific	No	Taylor and Yelland (2001)	Yes
EAST_TY_AWO_RPW	Eastern Pacific	Yes	Taylor and Yelland (2001)	Yes
WEST_TY_A_RPW	Western Pacific	No	Taylor and Yelland (2001)	Yes
WEST_TY_AWO_RPW	Western Pacific	Yes	Taylor and Yelland (2001)	Yes

3. Results and concluding remarks

Figure 2 shows the time series of calculated maximum wind speeds at 20-m height for the idealized vortex in the eastern North Pacific (Fig. 2a) and for the vortex in the western North Pacific (Fig. 2b). The calculated vortex intensified more rapidly in the eastern North Pacific than in the western North Pacific. The intensification was irrespective of the roughness length scheme. There was a notable difference in the wind speed variation: the intensification showed periodic fluctuations in the western North Pacific. The ocean coupling did affect the maximum wind speed in the eastern

North Pacific, while the coupling effect depended on the roughness length scheme in the western North Pacific. The rainpower effect helped lessen the vortex intensity without considering the ocean coupling effect, consistent with Sabuwala et al. (2015). However, the lessening effect was relatively small in the numerical experiments performed by the coupled model. Interestingly, the maximum wind speeds in the rainpower experiments did not decrease during the mature phase.

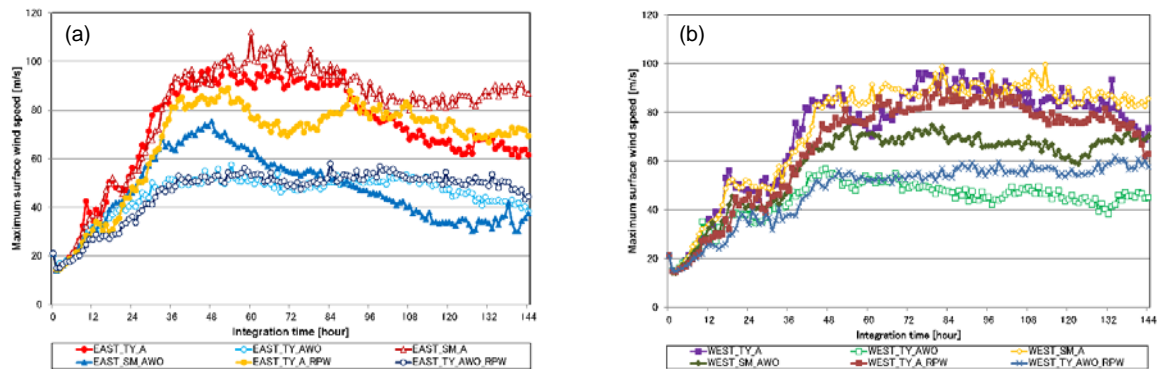


Figure 2 Time series of calculated maximum wind speeds at 20-m height (a) for the storm in the eastern North Pacific and (b) for the storm in the western North Pacific.

Figure 3 shows calculated storm positions relative to the initial position for the idealized vortex in the eastern North Pacific (Fig. 3a) and for the vortex in the western North Pacific (Fig. 3b). The vortex moved northwestward during the intensification phase (Fig. 2). It changed the moving direction cyclonically in the northern hemisphere. In the eastern North Pacific, the vortex's track was greatly sensitive to the roughness length scheme particularly in the experiment with the coupled model. In addition, the rainpower effect also affected the vortex's track. On the other hand, the effects of the roughness length scheme, ocean coupling and rainpower effect were relatively weak in the western North Pacific.

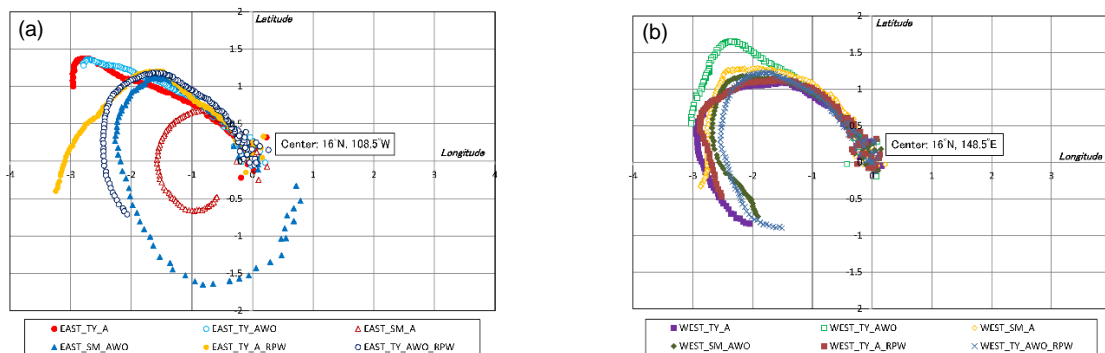


Figure 3 Storm positions relative to the initial position (a) for the storm in the eastern North Pacific and (b) for the storm in the western North Pacific.

The result of numerical experiments is consistent with Wada et al (2012): The vortex can intensify in the eastern Pacific more easily. However, the difference is relatively small in the numerical experiments by the coupled model. The difference of thermodynamic profiles does affect the intensity change of the vortex during the intensification phase particularly after the spin-up ends, around 18-hour integration time. The difference of the vortex's intensity might lead to the difference of the vortex's trajectory after the intensification phase. The sensitivity of the roughness length scheme, ocean coupling and rainpower effect to the trajectory shows various differences. For understanding the processes associated with the differences, the structural change and the asymmetric feature of the vortex should be examined in the future.

It should be noted that calculated mass fields such as the field of calculated sea-level pressures had an increasing or decreasing bias through the integration. The total mass in the computational domain was not conserved in this study. Apart from the necessity of the conservation, the configuration of the numerical experiments should be carefully examined to find a definite difference among the results of numerical simulations. In that sense, this report only shows a preliminary result of sensitivity numerical experiments.

Acknowledgement

This work was supported by MEXT KAKENHI Grant Number 15K05292.

References

- Bao, J.-W., J. M. Wilczak, J.-K. Choi and L. H. Kantha (2000). Numerical simulations of air-sea interaction under high wind conditions using a coupled model: A study of hurricane development. *Mon. Wea. Rev.*, 128, 2190-2210.
- Sabuwala, T, G Gioia, and P Chakraborty (2015). Effect of rainpower on hurricane intensity. *Geophys. Res. Lett.*, 42, 3024-3029.
- Smith, S. D., et al. (1992). Sea surface wind stress and drag coefficients: The HEXOS results. *Boundary Layer Meteorol.*, 60, 109-142.
- Taylor, P. K., and M. J. Yelland (2001). The dependence of sea surface roughness on the height and steepness of the waves. *J. Phys. Oceanogr.*, 31, 572-590.
- Wada, A. (2009). Idealized numerical experiments associated with the intensity and rapid intensification of stationary tropical cyclone-like vortex and its relation to initial sea-surface temperature and vortex-induced sea-surface cooling. *J. Geophys. Res. Atmos.*, 114, D18111.
- Wada, A., N. Kohno and Y. Kawai (2010). Impact of wave-ocean interaction on Typhoon Hai-Tang in 2005. *SOLA*, 6A, 13-16.
- Wada, A., N. Usui, and K. Sato (2012). Relationship of maximum tropical cyclone intensity to sea surface temperature and tropical cyclone heat potential in the North Pacific Ocean. *J. Geophys. Res. Atmos.*, 117, D11118.

Comparison of numerical simulations of Typhoon Haiyan in 2013 and Typhoon Mike in 1990

Akiyoshi Wada

Meteorological Research Institute, Tsukuba, Ibaraki, 305-0052, JAPAN

awada@mri-jma.go.jp

1. Introduction

In the previous report, Wada (2015) concluded that both subsurface warming in the northwestern Pacific Ocean and the ocean response to the Typhoon Haiyan (2013) should be taken into consideration to understand a rapid intensification of Haiyan and a resultant extremely strong intensity. Subsurface warming in the northwestern Pacific Ocean is an issue of the oceanic environmental conditions, while the ocean response, particularly sea surface cooling induced by a typhoon, depends on the intensity and translation as well as oceanic environmental conditions such as mixed layer depth, upper-ocean stratification and seasonal thermocline. In particular, it is difficult to investigate the sensitivity of the translation to typhoon simulations. Here we address Typhoon Mike (1990) which track is similar to Haiyan, but the translation is relatively slow so that we expect that the ocean response to Mike and the impact on the intensity would be quite different for two typhoons. In this report numerical simulations of typhoons Haiyan and Mike are compared.

2. Model and experimental design

Numerical simulations were performed for Haiyan and Mike by a nonhydrostatic atmosphere model and a coupled atmosphere-wave-ocean model. The coupled model (CPL) has been developed (Wada et al. 2010) based on the Japan Meteorological Agency nonhydrostatic atmosphere model (NHM). The computational domain for both typhoons was same as shown in Fig. 1 with a horizontal resolution of 2 km. Both CPL and NHM had 55 vertical levels with variable intervals from 40 m for the near-surface layer to 1013 m for the uppermost layer with the top height approaching nearly 26 km. The integration time was 84 hours (84 h) for Haiyan and 114 h for Mike with a time step of 4 seconds in NHM. The time step of the ocean model was 24 seconds, six times that of NHM. That of the ocean wave model was 10 minutes.

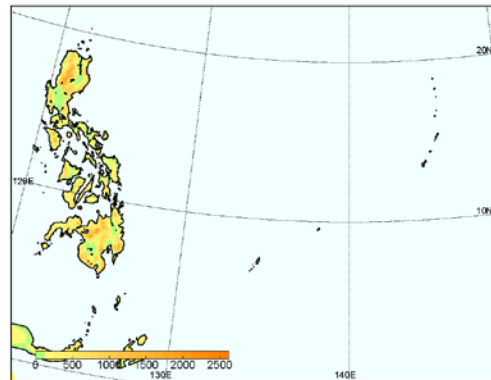


Figure 1 Computational domain with the horizontal resolutions of 2 km.

Physical processes used in the simulations were almost the same as applied in Wada et al. (2010) except for a sea spray parameterization (Bao et al. 2000) in the atmospheric surface-boundary layer. In particular, the the evaporation efficiency β was assumed equal to 1 when the 10-m wind speed exceeded 17 ms^{-1} and β linearly decreased as the wind speed became weak. The setting of β is similar to Bao et al. (2000), however, it was argued in Bao et al. (2000) that for extremely high winds, the droplet size may be so large that the droplets can fall back to the ocean before further evaporation extracts heat from the atmosphere, for which β approaches to zero. Oceanic initial conditions were obtained from the oceanic reanalysis datasets with a horizontal resolution of 0.5° calculated by the Meteorological Research Institute multivariate ocean variational estimation (MOVE) system (Usui, et al. 2006).

This study used the Japanese 25-year Reanalysis (JRA-25) (Onogi et al., 2007) and a subsequent reanalysis data set since 2005 (conventionally known as JCDAS) for producing atmospheric initial and lateral boundary conditions. Hereafter, JRA-25 and JCDAS are referred to simply as JRA-25.

3. Results and concluding remarks

Results of numerical simulations for Mike and Haiyan are shown in Fig. 2. The simulated track is reasonably simulated by both NHM and CPL compared with the best track for Haiyan and Mike, respectively (Fig. 2a). NHM tends to reproduce central pressures lower than the best-track central pressures. The typhoons simulated by NHM reach the minimum central pressure earlier than the best-track analysis, while the central pressures simulated by CPL tend to be still high compared with the best track central pressures (Fig. 2b).

The impact of the ocean coupling on the intensity of simulated typhoons is quite different for Haiyan and Mike. This is mainly caused by the difference in their moving speeds. In Fig. 2c, the moving speeds in Mike are slower than those in Haiyan in both simulations and best-track analysis.

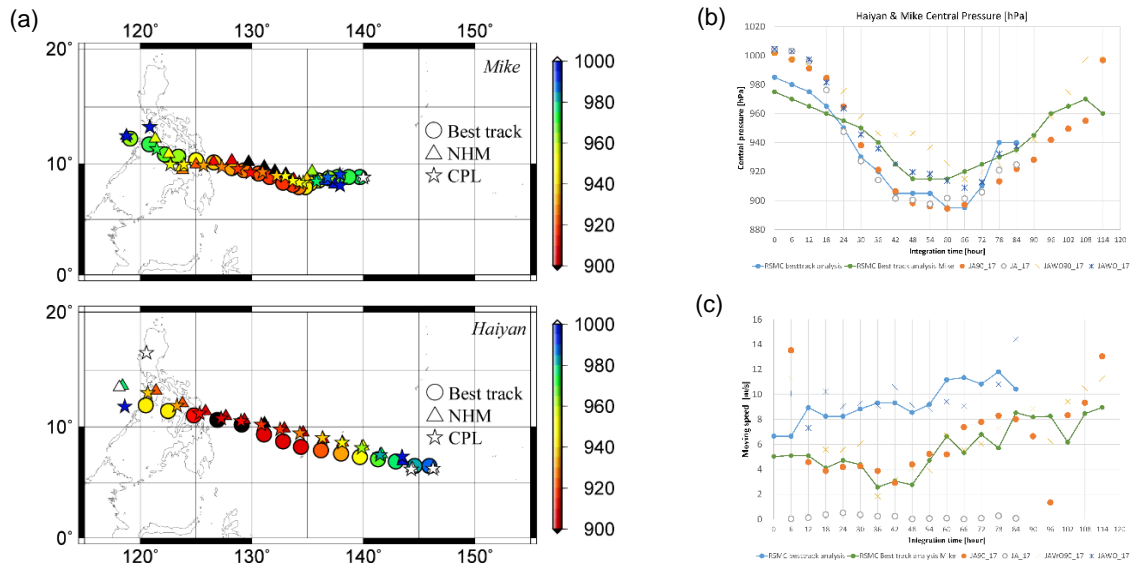


Figure 2 Results of numerical simulations with RSMC best-track data. (a) Simulated (triangles in NHM and stars in CPL) and best tracks with colors indicating central pressures for Mike (upper panel) and Haiyan (lower panel), (b) time series of simulated and best-track central pressures for Mike (green circles and orange crosses) and Haiyan (blue circles and crosses) and (c) as in Fig. 2b except for moving speeds.

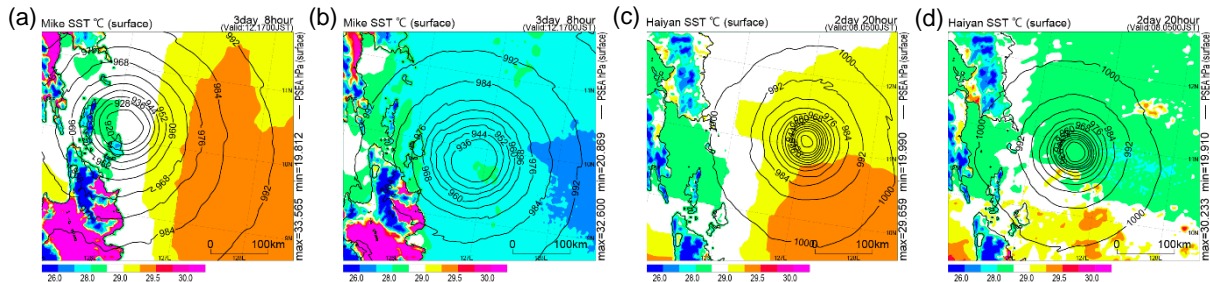


Figure 3 Horizontal distributions of central pressures at 8-hPa intervals (contour) and sea surface temperature (shades) at 70 h integration time for Typhoon Mike simulated by (a) NHM and (b) CPL and those at 68 h integration time for Typhoon Haiyan simulated by (c) NHM and (d) CPL.

The horizontal distributions of simulated sea surface temperature quite differs among the four experiments, two Mike's simulations and two Haiyan's simulations by NHM or CPL, respectively. Interestingly, the minimum central pressure for Mike simulated by NHM is comparable with that for Haiyan (Fig. 2b) even though the horizontal structure in the inner core quite differs between them. The difference of the minimum central pressure becomes remarkable between the simulations of Mike and Haiyan by CPL. The simulated central pressure increases from 36 h to 48 h (Fig. 2b) due to relatively slow moving speeds and resultant sea surface cooling (Fig. 2c). In fact, simulated sea surface temperature clearly decreases around the simulated Mike (Fig. 3b) compared with that around the simulated Haiyan (Fig. 3d). In other words, fast translation is responsible for rapid intensification and resultant maximum intensity of Haiyan. In addition, the area of cold wake represented by lowest sea surface temperature right behind the typhoon quite differs between Haiyan and Mike due to the difference of the size of simulated typhoon defined by the distance to the sharpest gradient of sea-level pressures from the typhoon center. In that sense, extremely intense Haiyan can be explained by fast translation, small size and relevant oceanic response to the typhoon. Subsurface warming in the northwestern Pacific Ocean is the second to explain the uniqueness of Haiyan.

Without coupling with the ocean model, the simulations for Mike and Haiyan show the similar minimum central pressures irrespective of the translation. However, the errors against the best track are quite different. In other words, the ocean response to a storm differs depending on the translation. In that sense, CPL will contribute to the improvement of TC intensity prediction for taking salient sea-surface cooling into account.

Acknowledgement

This work was supported by MEXT KAKENHI Grant Number 15K05292.

References

- Bao, J.-W., J. M. Wilczak, J.-K. Choi and L. H. Kantha (2000). Numerical simulations of air-sea interaction under high wind conditions using a coupled model: A study of hurricane development. *Mon. Wea. Rev.*, 128, 2190-2210.
- Usui, N., S. Ishizaki, Y. Fujii, H. Tsujino, T. Yasuda and M. Kamachi (2006). Meteorological Research Institute multivariate ocean variational estimation (MOVE) system: Some early results. *Advances in Space Research*, 37(4), 806-822.
- Wada, A., N. Kohno and Y. Kawai (2010). Impact of wave-ocean interaction on Typhoon Hai-Tang in 2005. *SOLA*, 6A, 13-16.
- Wada, A. (2015). Roles of the ocean on extremely rapid intensification and the maximum intensity of Typhoon Haiyan in 2013. *CAS/ISRC WGN Res. Activities in Atm. And. Oceanic Modelling*, 45, 9.10-9.11.

Typhoon Man-yi in 2013 simulated by an atmosphere-wave-ocean coupled model with 1.2-km horizontal resolution

Akiyoshi Wada

Meteorological Research Institute, Tsukuba, Ibaraki, 305-0052, JAPAN

awada@mri-jma.go.jp

1. Introduction

Previously, Wada (2015a) concluded for simulations on Typhoon Man-yi (2013) that deep warm water and a steep horizontal water-temperature gradient around the Kuroshio Current region were responsible for excitation of a mesovortex where the horizontal gradients of sea-level pressure and those of tangential winds were steep between the circulation center and the radius of the maximum surface wind. In addition, Wada (2015a) mentioned that rapid intensification of the mesovortex was triggered by the shift of the location of the mesovortex to inside the radius of the maximum surface wind. In order to verify the mechanism, numerical simulations are needed to be conducted by a nonhydrostatic atmosphere model with a horizontal resolution finer than 2 km (Wada, 2014, 2015a). The numerical model with the horizontal resolution less than 2 km is expected to more realistically reproduce a behavior of mesovortices excited inside the radius of the maximum wind speed and associated convective bursts. To that end, numerical simulations were performed by an atmosphere-wave-ocean coupled model (CPL) developed based on the Japan Meteorological Agency (JMA) nonhydrostatic atmosphere model (NHM) with a horizontal resolution of 1.2 km.

2. Model and experimental design

Numerical simulations for Typhoon Man-yi (2013) were conducted by both a regional nonhydrostatic model (NHM) and a regional atmosphere-wave-ocean coupled model (CPL) developed by Wada et al. (2010). Both models covered a ~ 2000 km x ~ 2400 km computational domain with a horizontal grid spacing of 1.2 km. Hereafter, 'A' indicates the results by NHM, whereas 'AWO' indicates the results by CPL. Both NHM and CPL had 55 vertical levels with variable intervals from 40 m for the near-surface layer to 1180 m for the uppermost layer. The top height was ~ 26 km. The simulations used the Japan Meteorological Agency global objective analysis data for atmospheric initial and boundary conditions (with a horizontal grid spacing of ~ 20 km) and the daily oceanic reanalysis data calculated by the Meteorological Research Institute multivariate ocean variational estimation (MOVE) system (Usui, et al. 2006) with the horizontal grid spacing of 0.1° . The initial time was 0000 UTC on 14 September in 2013. The integration time was 54 hours.

3. Results and concluding remarks

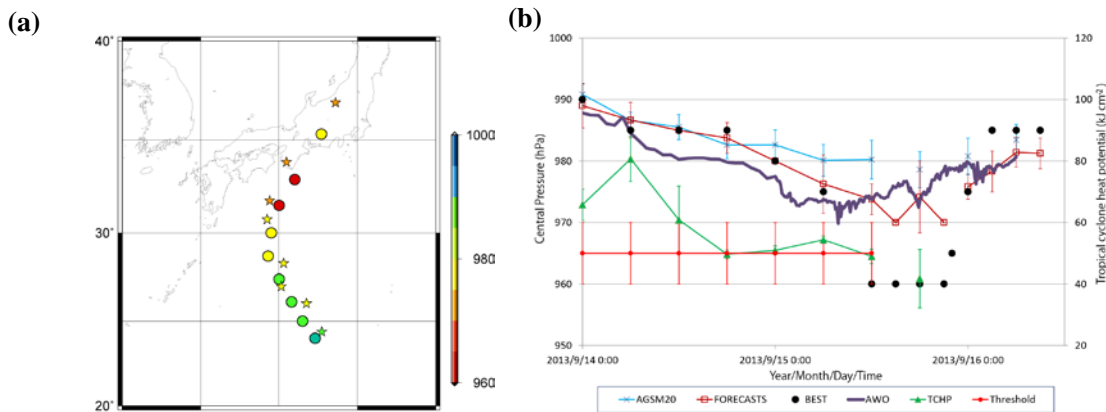


Figure 1 (a) The simulated track by CPL(\diamond) and the Regional Specialized Meteorological Center Tokyo best track (\circ) and (b) time series of simulated central pressure by CPL, the best-track central pressure, predicted central pressure by JMA global spectral model and forecast of central pressures together with tropical cyclone heat potential and the threshold.

Figure 1 shows the simulated track and the Regional Specialized Meteorological Center (RSMC) Tokyo best track positions every 6 hours (Fig. 1a) and the time series of central pressures simulated by CPL (Fig. 1b, AWO). Figure 1b also presents time series of the best-track central pressures (BEST), central pressures predicted by JMA global spectral model (AGSM20), and forecast of central pressures (FORECASTS) together with tropical cyclone heat potential (TCHP) and the threshold for intensification of a typhoon (Threshold) passed around 26° - 32° N (Wada, 2015b). It should be noted that the output intervals increase to 10 minutes after 24 h integration time from an 1-hour interval in order to capture the behavior of mesovortices.

The simulated track shows the westward bias with respect to the RSMC Tokyo best track. Simulated central pressures are relatively low compared with the best-track central pressures, central pressures predicted by JMA global spectral model and forecast of central pressures when the typhoon was south of 30°N over warm ocean with relatively high TCHP exceeding the threshold. In contrast, CPL could not simulate rapid intensification around 1200 UTC 15 September even though a local deepening occurred (Fig. 2).

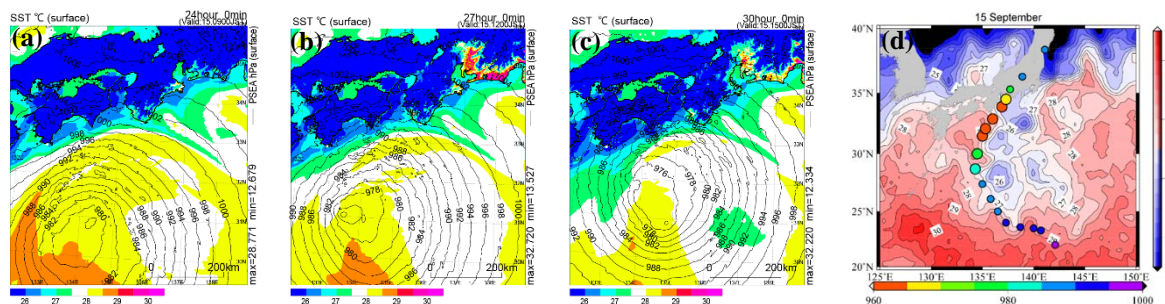


Figure 2 Horizontal distributions of sea surface temperatures (shades) with sea-level pressures (contours at 1-hPa intervals) at (a) 24 h, (b) 27 h and (c) 30 h integration times and (d) horizontal distribution of daily satellite sea surface temperature with a horizontal resolution of 0.25° (<http://www.remss.com/measurements/sea-surface-temperature>) with RSMC Tokyo best track with central pressures.

Figure 2 displays the horizontal distribution of sea surface temperature simulated by CPL from 24 h to 30 h every three hours with simulated sea-level pressures. On the right side of the simulated track, sea surface cooling is induced by the passage of the simulated typhoon Man-yi. The feature is also captured by daily satellite sea surface temperature (Fig. 2d). The inner core of the simulated typhoon passes over relatively warm ocean where the sea surface temperature exceeds 28°C, which is also similar to the relation of the best track to the horizontal distribution of daily satellite sea surface temperature. However, mesovortices within the inner core of the simulated typhoon are not exciting.

In order to understand why mesovortices within the inner core of the simulated typhoon are inactive, back trajectory analysis is conducted with 30 particles. The start point is at 31.35°N, 134.50°E, corresponding to the location of central pressure at 33 h integration time. The result is shown in Fig. 3. Near 31.35°N, 134.50°E, upward motion is analyzed. However, downward motion is also found on the south-eastern side from the center of the typhoon. The location corresponds to upshear-right side of the moving typhoon, not to down-shear sides. The relative location of the production of mesovortices to the vertical shear would be responsible for inactive mesovortex activities and resultant mesoscale convection.

This result suggests that high resolution less than 2 km is not always necessary to simulate a behavior of mesovortices. Fast translation compared with the best track would affect the simulation of the mesovortex behavior and thus typhoon intensity prediction.

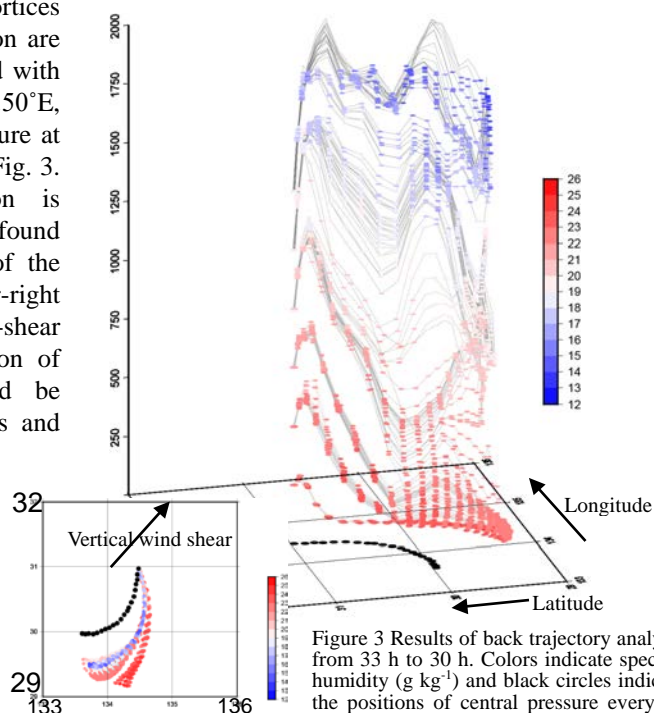


Figure 3 Results of back trajectory analysis from 33 h to 30 h. Colors indicate specific humidity (g kg^{-1}) and black circles indicate the positions of central pressure every 10 minutes.

Acknowledgement

This work was supported by MEXT KAKENHI Grant Number 15K05292.

References

- Usui, N., S. Ishizaki, Y. Fujii, H. Tsujino, T. Yasuda and M. Kamachi (2006). Meteorological Research Institute multivariate ocean variational estimation (MOVE) system: Some early results. *Advances in Space Research*, 37(4), 806-822.
- Wada, A., N. Kohno and Y. Kawai (2010). Impact of wave-ocean interaction on Typhoon Hai-Tang in 2005. *SOLA*, 6A, 13-16.
- Wada, A. (2014). Numerical simulations of Typhoon Man-Yi in 2013. *CAS/JSC WGNE Research Activities in Atmospheric and Oceanic Modelling*, 44, 9.07-9.08.
- Wada, A. (2015a). Unusually rapid intensification of Typhoon Man-yi in 2013 under preexisting warm-water conditions near the Kuroshio front south of Japan, *Journal of Oceanography*. DOI: 10.1007/s10872-015-0273-9
- Wada A. (2015b). Verification of tropical cyclone heat potential for tropical cyclone intensity forecasting in the Western North Pacific, *Journal of Oceanography*. DOI: 10.1007/s10872-015-0298-0

Extremely deepening of central pressures for Typhoon Neoguri in 2014 simulated by an atmosphere-wave-ocean coupled model and its dependency on the horizontal resolution.

Akiyoshi Wada

Meteorological Research Institute, Tsukuba, Ibaraki, 305-0052, JAPAN

1. Introduction

During 2014 typhoon season, Typhoon Neoguri made landfall over Kyushu late on 9 July. The typhoon was large and powerful with a minimum sea-level pressure of 930 hPa from 1800 UTC 6 to 0000 UTC 7 July according to the Regional Specialized Meteorological Center (RSMC) Tokyo best track data. However, the Japan Meteorological Agency (JMA) deterministic Atmospheric Global Spectral Model with a horizontal resolution of approximately 20 km (AGSM20) predicted a more extreme deepening of central pressures (Fig. 1).

The evolution of mean central pressure predicted by AGSM20 indicates that AGSM predicted central pressures were higher than the RSMC best-track central pressures until 0600 UTC on 7 July. Mean forecasts agreed with the best track central pressures better than the prediction. However, both AGSM20 predictions and JMA forecasts showed excess deepening of predicted central pressures after 0600 UTC on 7 July. For example, the time series of central pressures predicted by AGSM20 from the initial time at 1200 UTC on 4 July reveals that the minimum central pressure was 905 hPa, 25 hPa deeper than the best track minimum central pressure. In addition, the peak of minimum central pressure shifted one day afterward even though AGSM could not predict rapid intensification from 4 to 5 July.

2. Model and experimental design

It is known that typhoon-induced sea surface cooling helps suppress such kinds of excess intensification. Therefore, the purpose of this report is to verify the effect of typhoon-induced sea surface cooling on intensity predictions for Neoguri by using an atmosphere-wave-ocean coupled model with a horizontal resolution of 2 km. To examine the sensitivity of the horizontal resolution on the intensity predictions, sensitivity experiments were also performed with horizontal resolutions of 5 km and 10 km. The computational domain covers approximately 2400 km x 2800 km.

Numerical simulations were performed by a nonhydrostatic atmosphere model and a coupled atmosphere-wave-ocean model (Wada et al. 2010). The coupled model (CPL) has been developed based on the Japan Meteorological Agency nonhydrostatic atmosphere model (NHM). The horizontal resolution is shown in Table 1. Both CPL and NHM had 55 vertical levels with variable intervals from 40 m for the near-surface layer to 1013 m for the uppermost layer with the top height approaching nearly 26 km. The integration time was 84 hours (84 h) with a time step of 4 seconds. The initial time was 0000 UTC on 4 July in 2014.

The JMA global objective analysis data with a horizontal resolution of approximately 20 km was used for atmospheric initial and lateral boundary conditions. The latter was provided during the integration every 6 hours. The oceanic initial conditions except the sea surface temperature were obtained from the oceanic reanalysis datasets with a horizontal resolution of 0.5° calculated by the Meteorological Research Institute multivariate ocean variational estimation (MOVE) system (Usui, et al. 2006). Microwave optimally interpolated

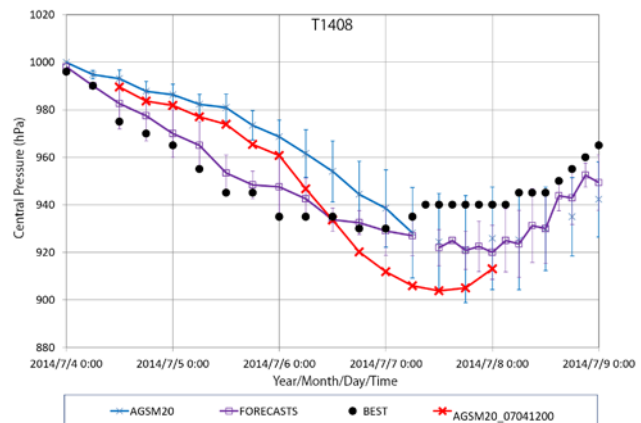


Figure 1 Time series of best-track central pressure (BEST), predicted mean central pressure by JMA global spectral model (AGSM20) and mean central pressure forecasts (FORECASTS) issued by JMA with the standard deviation during the typhoon every 6 hours, and that of central pressure predicted by AGSM20 from the initial time at 1200 UTC on 4 July (AGSM20_07041200).

Table 1 List of numerical experiments: acronym, model and horizontal resolution.

Acronym	Model	Horizontal resolution
A2km	NHM	2 km
A5km	NHM	5 km
A10km	NHM	10 km
AWO2km	CPL	2 km
AWO5km	CPL	5 km
AWO10km	CPL	10 km

sea surface temperature product with a horizontal grid spacing of 0.25° (<http://www.remss.com/measurements/sea-surface-temperature/>) was used as an initial condition for the sea surface temperature. In this study, no cumulus parameterization was used in conjunction with three-ice bulk cloud microphysics.

3. Results and concluding remarks

The simulated tracks showed marked northward biases from 126°E to 132°E during the middle of integration time. The typhoon positions predicted by AGSM20 and forecast positions became scattered around the Ryukyu chain, whereas simulated tracks became close to the RSMC best track positions (Fig. 2a). The impact of horizontal resolution on the track simulations is negligible during the early integration (Fig. 2b). However, the moving speed of storms in the experiments A5km and AWO10km tended to be relatively fast compared to that in the experiments A2km, AWO2km and that in the best track analysis. This is probably due to the setting of the parameter associated with lateral boundary condition.

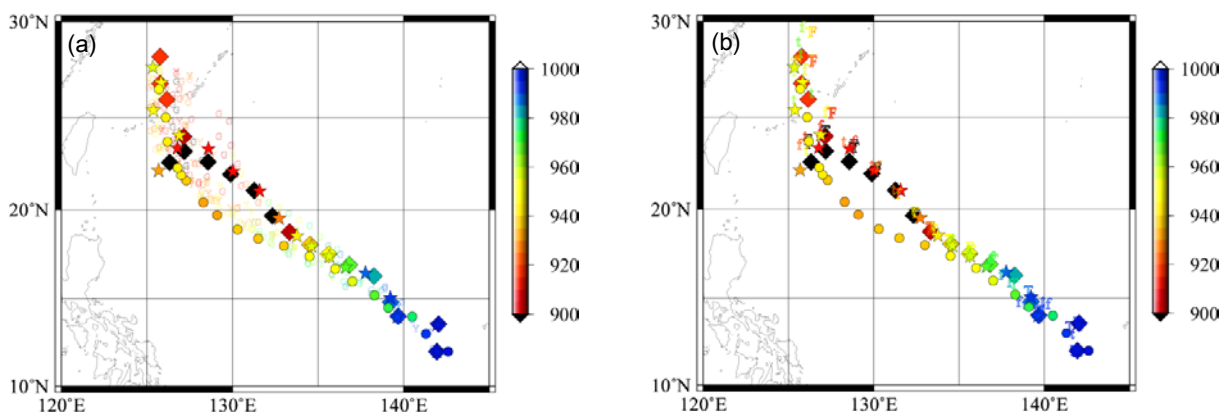


Figure 2 (a) Results of numerical simulations (◆:A2km, ★:AWO2km) with RSMC best-track data (●). The characters ‘G’ indicates predictions by AGSM20, while ‘Y’ indicates forecasts. (b) Same as (a) except for ‘F’ (A5km), ‘T’(A10km), ‘f’ (AWO5km) and ‘t’ (AWO10km) without ‘G’ and ‘Y’

Kanada and Wada (2015) reported that the appropriate horizontal resolution (~ 2 km) should be used to examine extremely intense TCs with extremely intensifying rates. In other words, it is expected that excess intensification could be suppressed by relatively coarse horizontal resolution. Figure 3 shows the time series of central pressures simulated in six experiments included in the difference of horizontal resolution and the difference between NHM and CPL. Even in the horizontal distribution of 10 km, however, the central pressure excessively deepened compared to the best track analysis even though CPL was used. The difference of central pressure simulations was relatively small compared with that between the horizontal resolutions of 5 km and 10 km, reported in Kanada and Wada (2015).

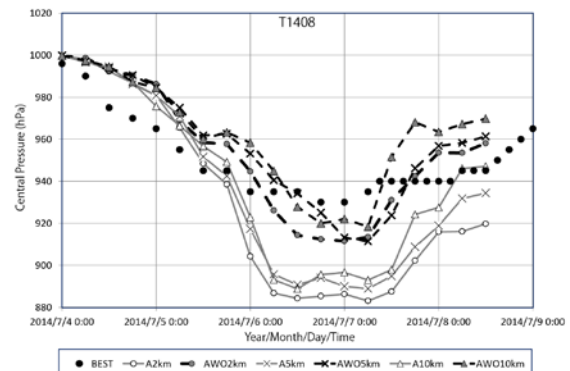


Figure 3 Time series of simulated central pressures in the experiments shown in Table 1.

Therefore, excessive intensification in the simulation of a typhoon is not completely suppressed by coarse horizontal resolution and typhoon-induced sea surface cooling simulated by an atmosphere-ocean coupled model. This is a lesson learnt by this study. In terms of the accuracy of central pressure, the accuracy of the best track central pressure has been a serious issue since there is less in situ observation in the vicinity of the center of typhoons in the western North Pacific than in the North Atlantic. Another issue is on the quality of global objective analysis data frequently updated depending on the upgrade of the system. Atmospheric initial and environmental conditions may affect simulated central pressures. These will be subjects in the future.

Acknowledgement

This work was supported by MEXT KAKENHI Grant Number 15K05292.

References

- Kanada, S. and A. Wada (2015). Sensitivity to horizontal resolution of the simulated intensifying rate and inner-core structure of Typhoon Ida, an extremely intense typhoon. *Journal of Meteorological Society of Japan*, 94A, 181-190.
- Usui, N., S. Ishizaki, Y. Fujii, H. Tsujino, T. Yasuda and M. Kamachi (2006). Meteorological Research Institute multivariate ocean variational estimation (MOVE) system: Some early results. *Advances in Space Research*, 37(4), 806-822.
- Wada, A., N. Kohno and Y. Kawai (2010). Impact of wave-ocean interaction on Typhoon Hai-Tang in 2005. *SOLA*, 6A, 13-16.